Molecular motors in new media

Lubbe, Anouk Sophia

Chapter 6: Solvent Effects on the Thermal Isomerization of a Rotary Molecular Motor

In this chapter, the thermal helix inversion of a second generation rotary motor is investigated in 50 solvents and solvent mixtures. A general trend of decreasing speed of rotation with increasing solvent viscosity is found, but this solvent parameter does not provide a full explanation for the observed effects. Statistical analysis is applied to reveal several solvent properties which influence speed of rotation.

This work was published as: A. S. Lubbe, J. C. M. Kistemaker, E. J. Smits, B. L. Feringa, *Phys. Chem. Chem. Phys.* 2016, *18*, 26725-26735.

6.1 Introduction

The term "solvent effects" comprises a large range of different solvent-solvent and solvent-solute interactions and is used to describe the combined effect of these interactions on chemical reactivity.[1] Even when the solvent is not participating in the reaction itself, solvent effects can be large and have therefore been studied in detail.[2] As the solvent is such an important part of any chemical reaction, its influence was already extensively studied in the 19th century. Pioneering work in the field was performed among others by Menshutkin,[3] Grunwald and Winstein,[4] Hammett and Deyrup,[5] and Hughes and Ingold,[6] but even after 150 years of extensive research, the nature of solvent effects remains elusive and its study of great importance. Recent examples include solvent effects in catalysis,[7] gelation,[8] regioselectivity in *ortho*-metallation,[9] radical reactions[10] and biomass conversion.[11] In unimolecular reactions, solvent effects are generally smaller but can comprise many different interactions. Therefore, for unimolecular reactions, a solvent scope can be used to gain insight in the effect of various solvent parameters. For example, significant solvent effects have been found in various thermal decomposition reactions,[12,13] ring inversion in cyclohexane,[14] the rotational relaxation of rod-like molecules,[15] and the fluorescence lifetime of rhodamine dyes[16]. The choice of solvent can even lead to different reaction mechanisms, as prominently observed in S_N1/S_N2 reactions,[6] or more recently in a denitrogenation reaction to form housane[17–19] and photodissociation in guaiacol.[20] Solvent effects on the photoisomerization of stilbene have been studied in detail.[21–23] The results have been explained using Kramers Theory.[24] Kramers theory states that in low-friction (low viscosity) media, the reaction rate increases with increasing friction. In medium-friction media the reaction rate will start to decrease with increasing friction until finally in high-friction media the reaction rate will approach the Smoluchowski limit, an inverse dependency on the solvent viscosity. Additionally, Gegiou *et al.* have argued that based on the free-volume model, this dependency should include a factor α (≤ 1), since only part of a molecule is required to move during an isomerization process.[25,26] This led to the following rate equation (in which η is the viscosity, and β is a fitting parameter):

$$\ln k = \beta - \alpha \ln \eta \qquad (6.1)$$

Related studies have been performed for the photoisomerization of diphenylbutadienes and azobenzenes, which show similar behavior.[22] Additionally, it is suggested that at low viscosities, solvent response frequencies are comparable to the reaction rate and that therefore medium effects other than viscosity may influence the reaction rate.[23,27] Especially in functionalized azobenzenes, a large effect of solvent polarity was observed for both the photochemical and the thermal isomerization.[28,29] For the latter, the influence of polarity on the rate was in fact much larger than the viscosity effect, which can be attributed to the significant change in dipole upon *cis* to *trans* isomerization. For example, the rate of the thermal *cis* to *trans* isomerization of an amine functionalized azobenzene was shown to be increased ~9000-fold by switching from cyclohexane to

DMF, despite the two having similar viscosities.[28] An investigation of the thermal and photochemical isomerization of bis-oxonols using twenty six different polar solvents showed that the thermal process is less sensitive to viscosity than the photochemical process, and that there is a marked difference in the response to protic and aprotic solvents.[30] Analogous to the observations for azobenzenes, the effect of a certain group of solvents on the thermal isomerization rate was significantly enlarged. For bis-oxonols these are protic solvents, which have a much larger interaction with the solute due to hydrogen bonding.

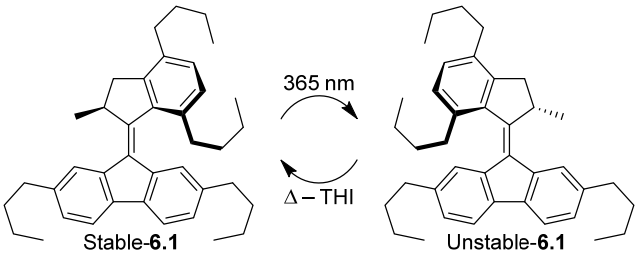

Scheme 6.1: Structure and isomerization processes of motor **6.1**. Photochemical *cis-trans* isomerization using UV-light to unstable-**6.1** and thermal helix inversion (THI) to stable-**6.1**.

For molecular motors, studies into solvent effects have so far been limited.[31,32] These compounds are structurally related to stilbenes, and it was indeed proven in a recent example that molecular motors obey the free-volume model.[33] However, opposed to stilbenes, rotary molecular motors readily undergo thermal isomerization. Additionally, none of the configurations a molecular motor can adopt has a significant dipole moment and no polar or hydrogen bonding substituent is required (Scheme 6.1). These structural properties make molecular motors ideal probes to study solvent effects, as they will not suffer from disproportionally large influences of specific solvents, such as observed for azobenzenes and bis-oxonols. These assumptions concur with the findings of Hicks *et al*,[34] who conclude that polarity can play a key role in isomerization dynamics, but that this effect is only significant when the process involves a large change in charge distribution. The influence of viscosity on the functioning of a second-generation molecular motor was investigated previously and determined to be large, but since the measurements were performed in only three solvents, no conclusion regarding any other solvent effects was reached.[35] In a recent publication, the influence of viscosity on the rate of the thermal isomerization of molecular motors was further investigated.[36] It was determined that this process can be described using Equation 6.1 and furthermore, that both α and β are viscosity and temperature dependent. This led to a reformulation of the Eyring equation, from which viscosity-dependent activation parameters could be obtained. However, the solvents in the previous investigation were limited to a range of linear alkanes. It is therefore impossible to reach any definite conclusions regarding solvent effects other than viscosity. In the current investigation, the rate of the thermal isomerization of an apolar second generation molecular motor has been studied in 50

solvents and solvent mixtures. The aim of this research was to gain a deeper understanding regarding the influence of solvent on this thermal isomerization process, especially regarding subtle effects which may have been overlooked in the past due to very large dipole-dipole or hydrogen bonding interactions. To achieve this goal, the most comprehensive solvent scope ever studied on a unimolecular thermal reaction is presented here.

6.2 Choice of molecular motor probe

The thermal helix inversion of molecular motor **6.1** was recently used in the study of viscosity effects on unimolecular thermal processes.[36] Its synthesis and characterization have been described in detail in this earlier publication. The motor was initially selected because of its *n*-butyl chains, which ensure high solubility in many solvents, and its equal mass balance around the central double bond leading to a similar displacement of both halves during isomerization. Additionally, the motor is apolar in all of its configurations, and during the thermal isomerization step (helix inversion) virtually no polarization is induced.[31] Therefore, we expect motor **6.1** to be almost inert to solvent-solute interactions, save for London dispersion forces and potentially some π-π stacking. Upon irradiation of motor stable-**6.1**, photoisomerization at its central double bond occurs, forming a diastereoisomer: unstable-**6.1**. In this diastereoisomer the stereogenic methyl group has adopted a pseudoequatorial rather than a pseudoaxial orientation. In this pseudoequatorial orientation, the methyl group induces significant steric strain due to its proximity to the fluorenyl moiety. Therefore this diastereoisomer is of an unstable nature. Unstable-**6.1** can release its steric strain through a thermally activated helix inversion. This thermal helix inversion (THI) converts unstable-**6.1** to stable-**6.1**' which is chemically identical to the initial configuration of stable-**6.1**. However, the motors upper half has undergone a 180 degrees unidirectional rotation with respect to its lower half. The motor is functionalized with long alkyl chains to ensure solubility in a wide range of solvents and no significant degradation was observed after several rotary cycles (Figure 6.1a). The THI can be monitored easily *via* UV-vis spectroscopy (Figure 6.1b). In a recent study, the activation parameters of the thermal helix inversion of motor **6.1** in a series of alkanes have been determined.[36] The obtained values of the half-life of unstable-**6.1** at 20 °C range from 331 sec in pentane to 555 sec in dodecane. This time scale is long enough for accurate measurements while still allowing for a large number of solvents to be scanned in a reasonable amount of time.

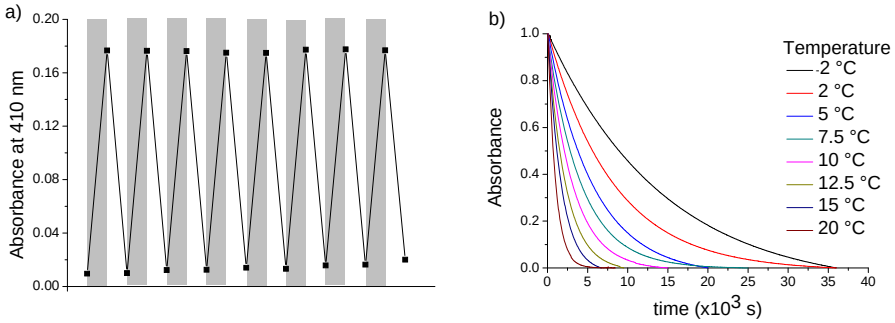

Figure 6.1: UV-vis studies of the THI of motor **6.1**. (a) Fatigue test. Irradiation with 365 nm light (grey areas) was followed by leaving the sample in the dark (white areas). (b) Normalized exponential decay lines from unstable-**6.1** to stable-**6.1** in methanol. Absorbance measured over time at 410 nm.

6.3 Results

50 Solvents divided over 11 solvent groups were studied, each of which was selected to elucidate the influence of a certain solvent property on the THI. Table 6.1 summarizes the results of the measurements. For 18 solvents and solvent mixtures a full Eyring plot has been constructed by measuring the duration of the THI at several temperatures (Figure 6.2) and the activation parameters are presented. For the other solvents and solvent mixtures the rate of the THI has been measured at 20 °C. For all solvents, the dynamic viscosity at room temperature has been determined in triplo using an Ubbelohde viscometer.

Solvent	ln k	ln η	Mol. wt	$t_{1/2}$ (min)	$\Delta^{\ddagger}H°$ (kJ mol^{-1})	$\Delta^{\ddagger}S°$ (J K^{-1} mol^{-1})	$\Delta^{\ddagger}G°$ (kJ mol^{-1})
Pentane	-6.172	-1.475	72.15	5.52±0.14	74.0±1.3	-43.6±4.7	86.8±0.1
Hexane	-6.221	-1.172	86.18	5.80±0.17	76.0±1.5	-37.4±5.2	86.9±0.1
Heptane	-6.299	-0.8896	100.2	6.28±0.17	80.4±1.5	-22.9±5.2	87.1±0.1
Octane	-6.388	-0.6127	114.2	6.87±0.18	76.0±1.4	-38.8±4.9	87.3±0.1
Nonane	-6.454	-0.3401	128.2	7.33±0.20	80.3±1.5	-24.6±5.1	87.5±0.1
Decane	-6.514	-0.09047	142.3	7.80±0.22	82.7±1.5	-17.0±5.3	87.6±0.1
Undecane	-6.603	0.1766	156.3	8.52±0.24	83.3±1.5	-15.6±5.4	87.9±0.1
Dodecane	-6.686	0.4069	170.3	9.25±0.27	80.6±1.8	-25.6±6.4	88.0±0.1
Dichloro methane	-6.386	-0.823	84.93	6.77±0.19	79.0±1.4	-28.5±4.9	87.3±0.1
Acetonitrile	-6.511	-1.017	41.05	7.72±0.24	84.6±1.5	-10.5±5.4	87.6±0.1
Methanol	-6.844	-0.4974	32.04	10.9±0.29	79.1±1.4	-32.0±5.1	88.4±0.1
10% Glycerol in methanol	-6.953	-0.1859	34.28	12.1			
20% Glycerol in methanol	-7.075	0.1912	36.85	13.7			

30% Glycerol in methanol	-7.221	0.6223	39.83	15.8			
40% Glycerol in methanol	-7.366	1.140	43.35	18.3			
50% Glycerol in methanol	-7.615	1.757	47.54	23.3±0.76	87.4±1.7	-9.9±6.1	90.3±0.1
15% Glycol in methanol	-6.998	-0.1612	34.55	12.6			
30% Glycol in methanol	-7.095	0.2499	37.48	13.9			
40% Glycol in methanol	-7.224	0.5570	39.73	15.9±0.43	83.0±2.7	-21.7±9.3	89.4±0.1
50% Glycol in methanol	-7.372	0.8727	42.26	18.4			
Ethanol	-6.984	0.1868	46.07	12.4±0.35	81.1±1.5	-26.4±5.2	88.8±0.1
1-Propanol	-6.975	0.7931	60.10	12.4			
1-Butanol	-6.883	1.089	74.12	11.3			
1-Pentanol	-6.882	1.425	88.15	11.3			
1-Hexanol	-6.929	1.697	102.2	11.8			
1-Heptanol	-6.981	1.988	116.2	12.4			
1-Octanol	-7.002	2.178	130.2	12.7			
1-Nonanol	-7.120	2.548	144.3	14.3			
Benzene	-6.869	-0.4246	78.11	11.1±0.37	85.6±2.4	-9.94±8.5	88.5±0.1
Toluene	-6.851	-0.5240	92.14	10.9			
Ethylbenz.	-6.843	-0.3943	106.2	10.8			
Butylbenz.	-6.874	0.05552	134.2	11.2			
Hexylbenz.	-6.944	0.5331	162.3	12.0			
Octylbenz.	-7.034	0.9579	190.3	13.1±0.39	87.5±1.6	-4.88±5.6	88.9±0.1
Dodecylben.	-7.240	1.721	246.4	16.1			
Para-xylene	-6.856	-0.4349	106.2	11.0			
Diethylbenz.	-6.941	-0.1555	134.2	12.0±0.48	83.7±2.0	-17.0±7.0	88.7±0.1
Dibutylbenz.	-7.080	0.8901	190.3	13.7±0.43	88.8±1.5	-0.676±5.5	89.0±0.1
Anisole	-7.074	0.1028	108.1	13.7			
Benzonitrile	-6.307	0.3231	103.0	6.33			
Anisol/ Benzonitrile	-6.586	0.1673	105.5	8.37			
Methyl benzoate	-7.159	0.7277	136.2	14.9			
Cyclopentane	-6.421	-0.8461	70.10	7.10			
Cyclohexan.	-6.486	-0.03315	84.16	7.57			
Cycloheptane	-6.524	0.4036	98.19	7.87			
Cyclooctane	-6.634	0.9245	112.2	8.78			
Isopentane	-6.060	-1.473	72.15	4.95			
Neohexane	-6.248	-1.008	86.17	5.97			

Methanol-d_4	-6.903	-0.4195	36.07	11.5
Methanol-d_1	-6.854	-0.4952	33.05	11.0

Table 6.1: Rate of thermal helix inversion (THI) of unstable **6.1**, viscosity, molecular weight and activation parameters for the 50 solvents and solvent mixtures investigated, including error margins. All values calculated to 20 °C and ambient pressure.

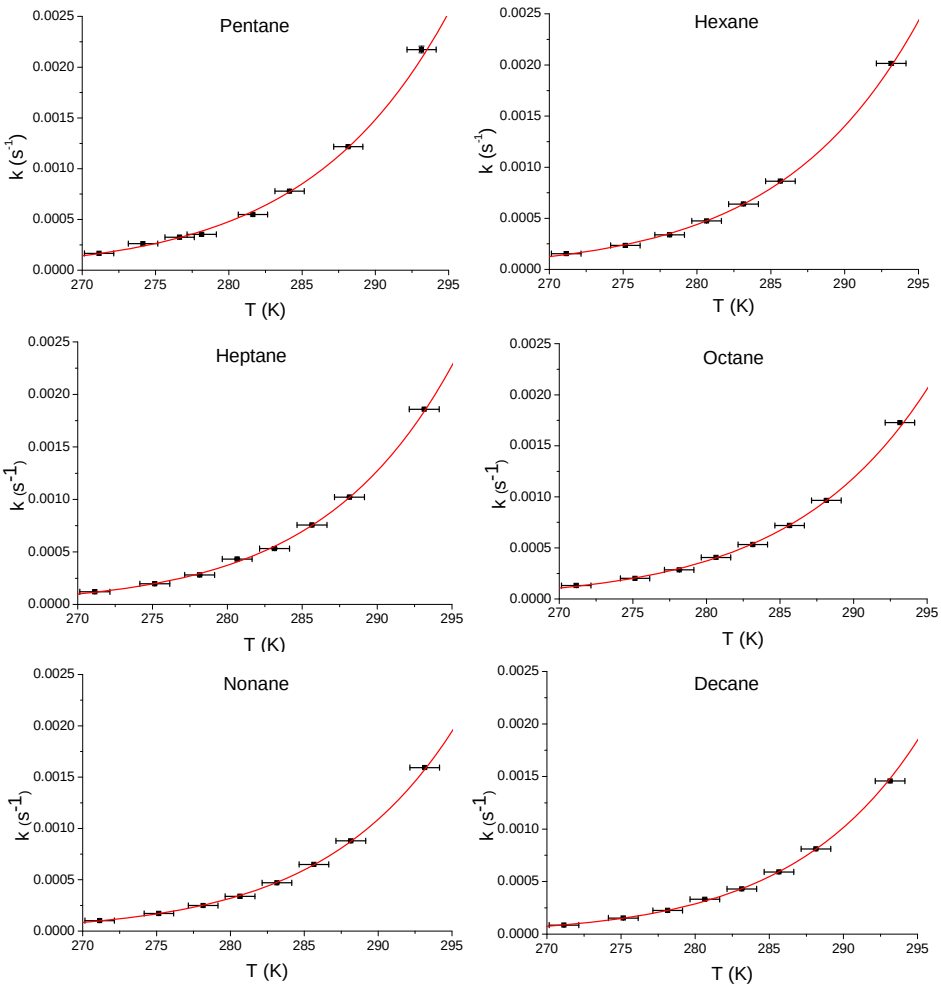

Figure 6.2: Eyring plots for the THI of motor **6.1**, recorded in 18 different solvents.

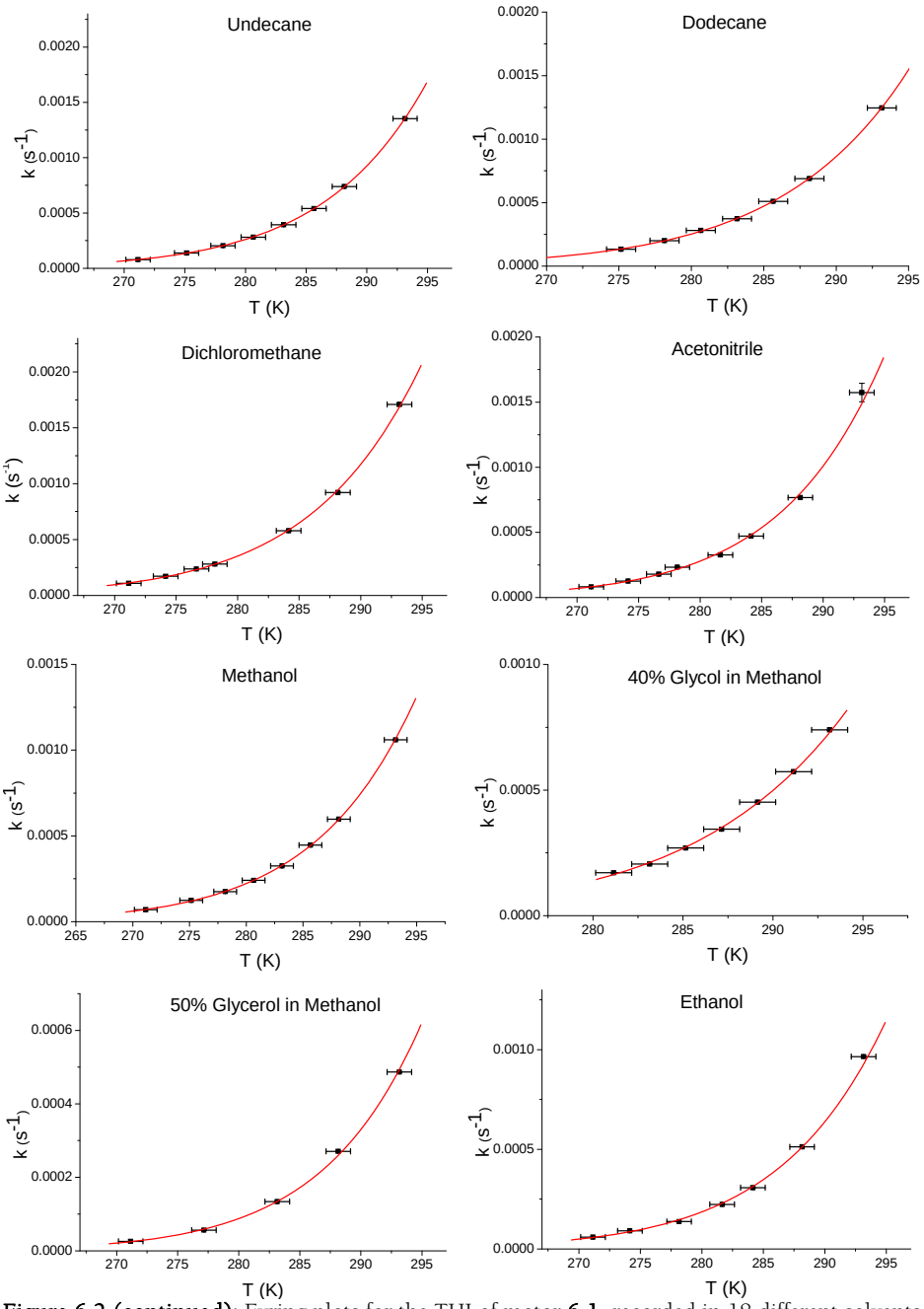

Figure 6.2 (continued): Eyring plots for the THI of motor **6.1**, recorded in 18 different solvents.

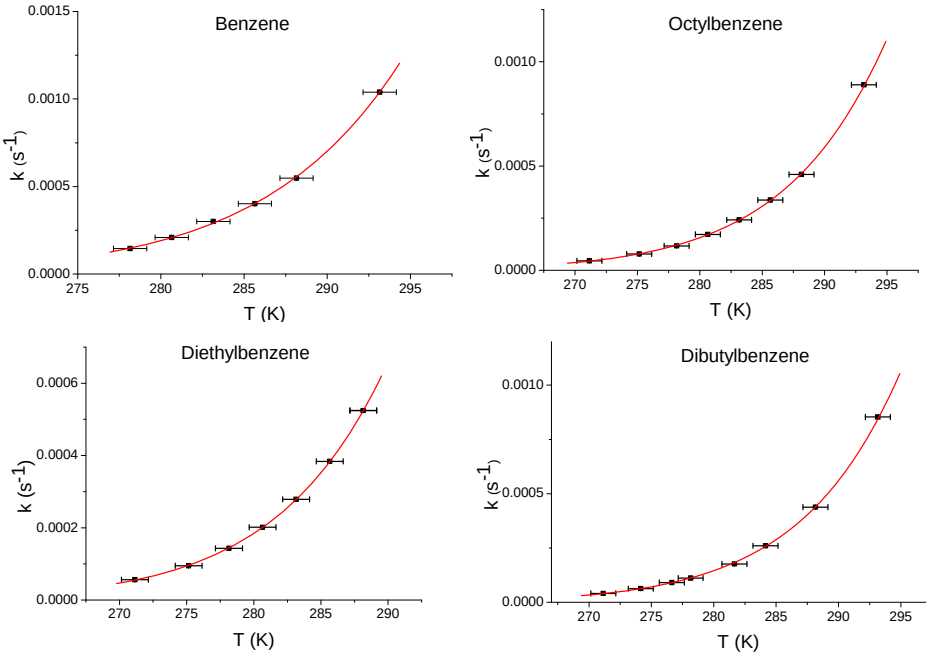

Figure 6.2 (continued): Eyring plots for the THI of motor **6.1**, recorded in 18 different solvents.

6.3.1 Polar solvents

Following the series of alkanes previously investigated, our initial investigations aimed at polar solvents. Figure 6.3 shows the natural log of the rate of the THI at 20 °C, versus the natural log of the dynamic viscosity at the same temperature for several solvents. The black squares represent a series of alkanes, starting from pentane (top left) to dodecane (bottom right). As free volume theory predicts, these points form a straight line (R^2 = 0.994, Pearson's r = -0.997).[25] A detailed analysis of these results can be found in our earlier work ($\alpha°$ = 0.275 and $\beta°$ = –6.55).[36,*] The blue triangles represent mixtures of methanol and glycerol, starting from pure methanol (top left) to 50 wt % glycerol in methanol (bottom right). Because the dipole moments of methanol and glycerol are so similar (resp. 2.87 D and 2.56 D),[37] this group of solvent mixtures represents a very close approximation of a perfectly homologous series of solvents with increasing viscosities and constant polarity (analogous to the homologous series of alkanes which also possesses constant polarity over increasing viscosity). The glycerol/methanol mixtures behave quite similar to the alkane series (R^2 = 0.998, Pearson's r = -0.999). Rate decreases when viscosity increases as predicted by Kramers theory for high-friction media (i.e. a liquid).[24] According to Schroeder, this linear relation indicates that the macroscopic viscosity is proportional to the microscopic friction around the solute.[21] Howev-

[*] Standard state (°) equals room temperature (20 °C) and atmospheric pressure (1 atm).

er, the THI process of unstable-**6.1** in the glycerol/methanol series as a whole is significantly slower (has a larger negative β value) than in the alkane series ($\alpha^\circ = 0.335$ and $\beta^\circ = -7.01$, vs $\alpha^\circ = 0.275$ and $\beta^\circ = -6.55$, respectively). Additionally, the rate of the THI of motor **6.1** was measured in dichloromethane and acetonitrile (Figure 6.3, unfilled and filled red circle, respectively). Dichloromethane (dipole moment 1.14 D) lies more or less in the alkane series and acetonitrile (dipole moment 3.44 D), although significantly more polar than methanol and glycerol, lies only slightly above the extrapolated trend line for the glycerol/methanol series. Because there is no change in polarization during the isomerization process, these results are within our expectations.

Polarity is not the only difference between the alkane series and the glycerol/methanol series. Methanol and glycerol are excellent hydrogen bond donors and acceptors and their hydrogen bond forming ability per mass unit is very similar (methanol: 1 hydroxy group per 32.04 u, glycerol: 3 hydroxy groups per 92.09 u; equals 1 hydroxy group per 30.70 u). Therefore, the overall hydrogen bonding ability of the mixture does not change significantly upon increasing viscosity by varying the ratio of the components. This is in accordance with the linear increase of the natural log of *k* with an increasing natural log of the viscosity. Dichloromethane is both a poor hydrogen bond donor and acceptor, whereas acetonitrile is a fairly good hydrogen bond acceptor, which explains why in these solvents, the rate of the THI of motor **6.1** is lower than in the alkanes, but higher than in the glycerol/methanol series. A similar conclusion was reached by Benniston and Harriman, who report the rate of the thermal isomerization step of bis-oxonols in 26 different solvents.[30] They see a marked difference between protic and aprotic polar solvents and deduce that hydrogen bonding to the bis-oxonol is responsible for the retardation. However, no mechanistic studies have been performed to confirm that solvent-solvent hydrogen bonding is not also partly responsible for the decrease in rate.

Motor **6.1** is a very apolar molecule and will have little or no hydrogen bonding itself to the solvent, yet hydrogen bonding appears to be the predominant factor in the difference in the rates of the THI. Therefore, it is implied in the current study that in this system, for the solvents studied thus far, solvent-solvent interactions rather than solvent-solute interactions have a much larger influence on the rate. In other words, the THI should be considered in a 'solvent-shell' type approach, as due to solvation, the solvent forms a shell around the molecule.[1,38] During the THI, the molecule is required to undergo a major rearrangement, which means that the solvent shell needs to rearrange as well. If intermolecular forces in the solvent are strong, for example due to hydrogen bonding, this rearrangement requires more energy input, thereby decelerating the motor rotation. These interactions will dominate the solvent effects upon thermal isomerization, since solvent-solute interactions appear to be minimal. This is in contrast with results found for azobenzenes, which are polar and therefore dominated by effects based solvent polarity.[28,29] In the current example, solvent-solute effects may still influence the rate. For example, weak hydrogen bonding of the solvent to the aromatic rings

of motor **6.1** can be envisioned.[39] However, since the overall dependence on viscosity is retained, these effects are of a much smaller magnitude than observed for more polar switches.

6.3.2 Polar solvents II and alcohols

An additional set of solvents was measured in order to elucidate the differences between the solvent groups. Figure 6.3 shows the results of these measurements. A series of *n*-alcohols confirms our assumptions regarding the importance of the hydrogen bonding ability, clearly exhibiting a non-linear trend (Figure 6.3, turquoise diamonds, R^2 = 0.412, Pearson's r = -0.642). While rates in low-weight alcoholic solvents such as methanol ($\ln k$ = -6.84) and ethanol ($\ln k$ = -6.98) are significantly retarded compared to aliphatic solvents of similar viscosity (resp. octane ($\ln k$ = -6.39) and undecane ($\ln k$ = -6.60)), the alcohol series is converging towards the alkane series with increasing molecular weight. This is to be expected since large *n*-alcohols have an increasing aliphatic character with dispersion interactions dominating, and intermolecular hydrogen bonding is much reduced.

The data set of the glycerol/methanol mixtures was extended by measurements performed in glycol/methanol mixtures. Glycol has a very similar hydrogen bonding ability per mass unit (1 hydroxy group per 31.035 u) compared to methanol and therefore THI rates in these mixtures were expected to be similar to those in the glycerol/methanol series. As can be seen in Figure 6.3 (pink crosses), the data indeed fits well on the glycerol/methanol trend line (combined methanol/glycol/glycerol series: R^2 = 0.987, Pearson's r = -0.993).

If hydrogen bonding is indeed the reason that rates are much slower in the methanol/glycol/glycerol series than in the alkane series, changing the nature of the hydrogen bond might give an insight into the mechanism behind this rate retardation. Hydrogen and deuterium are electronically identical, and therefore it is often assumed that hydrogen bonds and deuterium bonds are identical.[40] However, their mass and therefore their vibrational energy are different. Calculations suggest that deuterium bonds can be slightly stronger than hydrogen bonds, with an energy difference of up to 1.3 kJ mol^{-1}.[40,41] The rate of the THI of motor **6.1** was therefore measured in both CD_3OD and CH_3OD (Figure 6.3, green pluses). The result for CH_3OD was nearly identical to the result for methanol. The isomerization rate was slightly lower in CD_3OD, but this is expected due to its slightly lower viscosity. No additional conclusions can be obtained from these results, since a significant kinetic isotope effect appears absent.

6.3.3 Aromatic solvents

Subsequently aromatic solvents were investigated. Motor **6.1** has a large aromatic core, and therefore solvent-solute interactions other than those previously observed were expected. The rate was measured in two solvent series: alkylbenzenes (Figure 6.3, purple squares, R^2 = 0.922, Pearson's r = -0.960), and *para*-dialkylbenzenes (Figure 6.3, grey circles, R^2 = 0.972, Pearson's r = -0.986). Surprisingly, the rates in these solvents are much closer to those for the glycerol/methanol series than the alkane series. Benzene ($\ln k$ = -6.87), toluene ($\ln k$ = -6.85), ethylbenzene ($\ln k$ = -6.84) and para-xylene ($\ln k$ = -6.86) all behave almost identical to methanol ($\ln k$ = -6.84). Just as seen for the alcohol series, towards longer alkyl chains both of these groups seem to converge to the alkane line which can be explained by the increasing aliphatic character of the solvents as molecular weight increases. Due to π-π stacking, intermolecular forces are expected to be much stronger in aromatic solvents than in aliphatic solvents, which is consistent with a solvent shell theory.[42] However, due to the aromatic nature of motor **6.1**, solvent-solute interactions could be of more importance in these aromatic solvents.

To further investigate the influence of π-π interactions on the rate, the THI was measured in anisole, benzonitrile, and a 1:1 mixture of the two (Figure 6.3, filled orange triangles). These two solvents have a very similar viscosity but a very different electronic configuration. In benzonitrile ($\ln k$ = -6.31) the unstable isomer has a much shorter half-life than in anisole (ln k = 7.07), and in fact than in all other aromatic solvents. Many explanations regarding the remarkably different behaviour of motor **6.1** in benzonitrile were considered. The most likely is the theory that there are more solvent-solute interactions in the aromatic solvents i.e. π-π interactions, and that the transition state of the isomerization process can therefore be affected more strongly by the solvent. In the transition state, the butyl chain on the upper half of motor **6.1** is compressed against the lower half of the motor,[36] leading to a temporary increase in electron density. Interaction with the electron poor benzonitrile would relieve some of this electron density, thereby stabilizing the transition state and increasing the reaction rate, which would explain the difference between benzonitrile and the relatively electron-rich anisole and alkylbenzenes. This explanation would indicate a combination of dipole moment and possibly other solvent effects, but only affecting the isomerization when π-π stacking can occur. Such complex interactions are outside the scope of this research, but would certainly warrant further investigations. As a control, a different electron-poor aromatic solvent, methyl benzoate (Figure 6.3, unfilled orange triangle, $\ln k$ = -7.16), was measured. The data are in line with the results from the other aromatic solvents, which might indicate that electron density on the aromatic ring is irrelevant to the THI, leaving benzonitrile a solitary, inexplicable outlier from the aromatic solvent trend line.

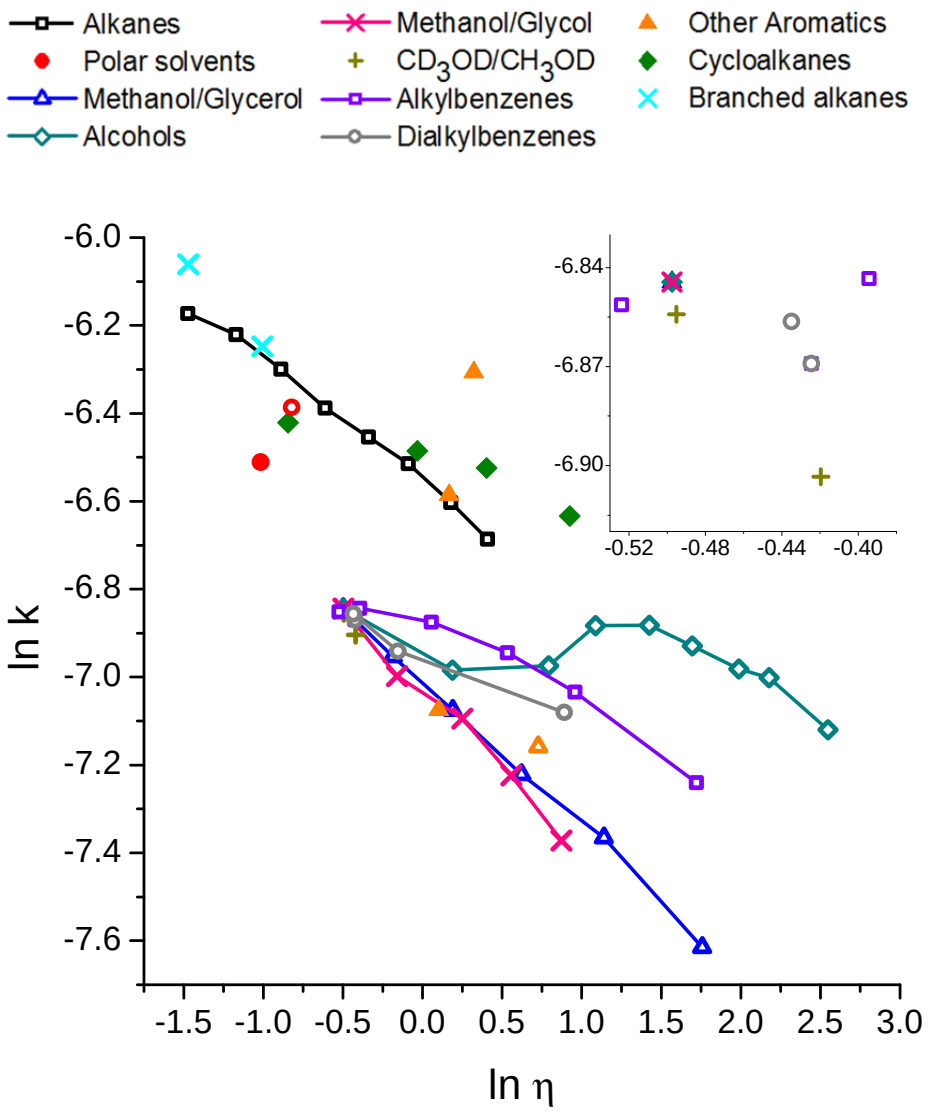

Figure 6.3: ln *k* versus ln η for a series of alkanes (black squares), alcohols (turquoise diamonds), methanol/glycerol mixtures (blue triangles), methanol/glycol mixtures (pink crosses), monoalkyl aromatic solvents (grey circles), dialkyl aromatic solvents (purple squares), deuterated methanols (green pluses), polar solvents (red circles), electron rich or poor aromatic solvents (orange triangles), a series of cycloalkanes (green diamonds), branched alkanes (light blue crosses. For clarity, lines are given to guide the eye. A zoom-in of a crowded area of the graph is included in the top right corner.

6.3.4 Cycloalkanes and branched alkanes

Finally, the rate of the THI of motor **6.1** was determined in several cyclic (green diamonds) and branched (cyan crosses) alkanes (Figure 6.3). Of the branched alkanes, neohexane (ln k = -6.248) lies on the alkane line. Isopentane (ln k = -6.060) has a similar viscosity to pentane but lies above the line due to a slightly faster THI. Not much can be concluded regarding the α value based on 2 data points, but for the thermal isomerization of bis-oxonols Benniston and Harriman[30] find that the α value is very different for branched alkanols than for linear alkanols. However, they attribute this effect to steric blocking of the hydroxy group. The deviation of isopentane from the alkane line might simply be a result of weaker Van der Waals interactions within the solvent, as is apparent from the difference in cohesive energy density between isopentane (45.6 J cm^{-3}) and *n*-pentane (47.7 J cm^{-3}).[43] This could lead to a less dense solvent shell and therefore a lower barrier for the THI.

The cycloalkanes (Figure 6.3, green diamonds, R^2 = 0.930, Pearson's r = -0.965), ranging from cyclopentane to cyclooctane, lie in the same region as the linear alkanes. This solvent group is not expected to have a linear trend. The smallest cycloalkane (cyclopentane) is very rigid, but with every methylene expansion the ring increases significantly in flexibility, i.e. degrees of freedom. Therefore, it seems likely that much larger cycloalkanes would ultimately behave as linear alkanes, whereas the small rings might exhibit a different behaviour. Cyclopentane (ln k = -6.421) for example, lies below the alkane line. Analogous to isopentane, the rate might in this case be lower than expected based on viscosity due to the highly rigid structure of cyclopentane, which could lead to a relatively tightly ordered solvent shell.

6.4 Correlation of rate to other solvent effects

While viscosity and possibly hydrogen bonding and π-π interactions in the solvent explain most of the general trends observed in the graphs above, there are clearly other solvent effects that influence the rate of the THI. In an effort to elucidate these effects, the rate of the THI has been compared to 8 solvent parameters:[43–48] the Kamlet-Taft parameters for the hydrogen bond donating and accepting ability (α and β, respectively), two different polarity scales (π^* and $E_T(30)$), the dielectric constant ε, the surface tension (ST), the cohesive energy density (c.e.d.) and the diffusion coefficients (D) of motor **6.1**. The diffusion coefficients have been measured by DOSY-NMR, while the other solvent parameters were obtained from the literature. The combined data are summarized in Table 2.[†]

[†] These solvent parameters are not available for the glycerol/methanol, glycol/methanol and anisole/benzonitrile mixtures and could also not be found for cycloheptane, 1-heptanol, dodecylbenzene, neohexane and the deuterated solvents.

Figure 6.4 shows ln k for the THI of motor **6.1** plotted against the eight solvent parameters. These parameters reflect solvent properties that might back up the theory regarding the importance of hydrogen bonding and/or π-π interactions, and on the other hand shed light on the unexplained behaviour that has been observed in several solvents. The parameters are not known for the glycerol/methanol and glycol/methanol mixtures used. However, comparison with other solvent groups might give some useful insight. A statistical analysis was performed on the datasets to avoid any biased interpretation. The coefficient of determination (R^2) was calculated for all specific solvent groups for the linear relationship of ln η vs ln k. To determine the linearity of this relationship the Pearson product-moment correlation coefficient (Pearson's r) was calculated and reported with its probability (p-value). The sign indicates the direction of the trend, zero signifies complete randomness and |1| signifies a perfect linear relationship. Pearson's r values ≥ |0.708| mean that more than 50% of the variance is related, Pearson's r values ≥ |0.995| mean that more than 99% of the variance is related; p-values < 0.01 indicate a significant relationship. Where the Pearson correlation coefficient (r) is appropriate to evaluate the linear relationship between ln k and ln η, it is not expected *a priori* of the other datasets to be linear. Therefore, the Spearman's rank correlation coefficient (ρ) was used to assess the presence of a monotonic relationship between the rate and the different solvent parameters. For example, the individual solvent groups exhibited strong linear relationships, indicated by very high Pearson correlations (r > 0.95 for all solvent groups except linear alcohols). However, when ln k vs. ln η is assessed as a whole, its linear relationship is less evident (r = -0.689). Nonetheless, the complete dataset does exhibit a significant strong monotonic relationship (ρ = -0.728).

Solvent	Sym.	ln k	π^{*}[44,45]	ε[46]	$E_T(30)$[46]	α[44,45]	β[44,45]	ST[47] (mN m^{-1})	D	c.e.d.[48,43] (J cm^{-3})
Pentane	■	-6.172	-0.08	1.84	30.9	0	0	16.1	17.93	47.7
Hexane	■	-6.221	-0.08	1.89	30.9	0	0	18.4		52.8
Heptane	■	-6.299	-0.08	1.94	30.9	0	0	21.1	11.00	56.3
Octane	■	-6.388	0.01	1.95	31	0	0	21.6		56.9
Nonane	■	-6.454		1.97	30.8			22.9		
Decane	■	-6.514	0.03	1.99	30.8	0	0	23.8		59.9
Undecane	■	-6.603						24.7		
Dodecane	■	-6.686	0.05	2.10	31	0	0	24.5	2.500	61.2
Dichloro methane	○	-6.386	0.82	9.02	40.7	0.13	0.10	27.8	11.28	97.5
Acetonitrile	●	-6.511	0.75	36.0	45.6	0.19	0.31	29.3		143
Methanol	◆	-6.844	0.60	33.6	55.4	0.93	0.62	22.5	8.719	204
Ethanol	◆	-6.984	0.54	25.0	51.8	0.83	0.77	22.4		168
1-Propanol	◆	-6.975	0.48	21.5	50.5	0.76	0.84	23.7		143
1-Butanol	◆	-6.883	0.47	18.4	49.7	0.79	0.88	25.4		122

1-Pentanol	◆	-6.882	0.40	15.8	49.3	0.84	0.86	25.8	1.386	
1-Hexanol	◆	-6.929	0.40	14.4	48.9	0.8	0.84	26.2		
1-Octanol	◆	-7.002	0.40	10.3	48.3	0.77	0.81	27.5		
1-Nonanol	◆	-7.120						28.3	0.425	
Benzene	■	-6.869	0.59	2.40	34.3	0	0.10	28.9	7.427	84.1
Toluene	■	-6.851	0.54	2.43	33.9	0	0.11	28.5	7.425	79.3
Ethylbenz.	■	-6.843						29.3		76.3
Butylbenz.	■	-6.874						29.2		
Hexylbenz.	■	-6.944						30.0		
Octylbenz.	■	-7.034							1.724	
Para-xylene	●	-6.856	0.43	2.27	33.1	0	0.12	28.6		79.2
Diethylbenz.	●	-6.941						29.0		
Dibutylbenz.	●	-7.080							2.032	
Anisole	▲	-7.074	0.73			0	0.32	35.7	4.339	
Benzonitrile	▲	-6.307	0.90	25.3	41.5	0	0.41	39.4	5.544	
Methyl benzoate	△	-7.159			38.1	0	0.39	37.8		
Cyclopentane	◆	-6.421						22.6		65.6
Cyclohexane	◆	-6.486	0	2.02	30.8	0	0	25.2		66.9
Cyclooctane	◆	-6.634						29.8		
Isopentane	✕	-6.060								45.6

Table 6.2: 8 Different solvent parameters[‡] of 33 solvents, plus the symbols used to depict the solvents in Figure 6.4.

Figure 6.4a, b and c show 3 different parameters related to polarity. In Figure 6.4a this is π*, a polarity scale based on solvatochromism.[49] This scale is based on several dyes and gives a measure of the extent to which a solvent stabilizes ionic or polar solutes. As motor is **6.1** neither ionic nor polar, any correlation found on this scale must be treated with caution. However, the position of the polar and some aromatic solvents on this scale relative to the alcohols indicates that there is no obvious relation between the π* scale and ln *k* evident from a very weak Spearman's correlation (ρ = -0.345). In Figure 6.4b, ln *k* is plotted against the dielectric constant, ε. This parameter reflects dipoles, polarizability and hydrogen bonding sites and is therefore a relevant measure of polarity. In this plot, the alcohol solvent group is again seen ranging from a high value on the x-axis (for methanol) to much lower values upon increasing the aliphatic tail length. All aliphatic and apolar aromatic solvents have a dielectric constant < 5, and any other solvents are more or less randomly distributed over the graph (ρ = -0.571).

[‡] Solvent parameters are the solvatochromism scales π* and $E_T(30)$, the dielectric constant ε, the Kamlet-Taft parameters for hydrogen bonding ability (α) and hydrogen donating ability (β), the surface tension (ST), the diffusion constant D and the cohesive energy density (c.e.d.).

Finally, Figure 6.4c shows the $E_T(30)$ solvatochromism scale.[50] Out of the three polarity scales, this is the only one that plots dichloromethane and acetonitrile between the aliphatic solvents and the alcohols, where they would be expected if a correlation between $E_T(30)$ and ln *k* existed. Otherwise, this plot looks very similar to Figure 6.4a and b and exhibits a slightly better but still only moderate correlation (ρ = -0.629). Clearly the aliphatic and alcoholic groups stay well separated from each other on all polarity scales. However, within the alcoholic group or with respect to the other solvents under investigation, no clear correlation between the rate and solvent polarity has been observed. This is expected since it can be rationalized that the retardation in alcohols was specifically due to their hydrogen bond donating ánd accepting properties, while for aromatic solvents the retardation stems from their π-π solvent-solvent interaction. Both effects have a different origin than the polarity of the solvent.

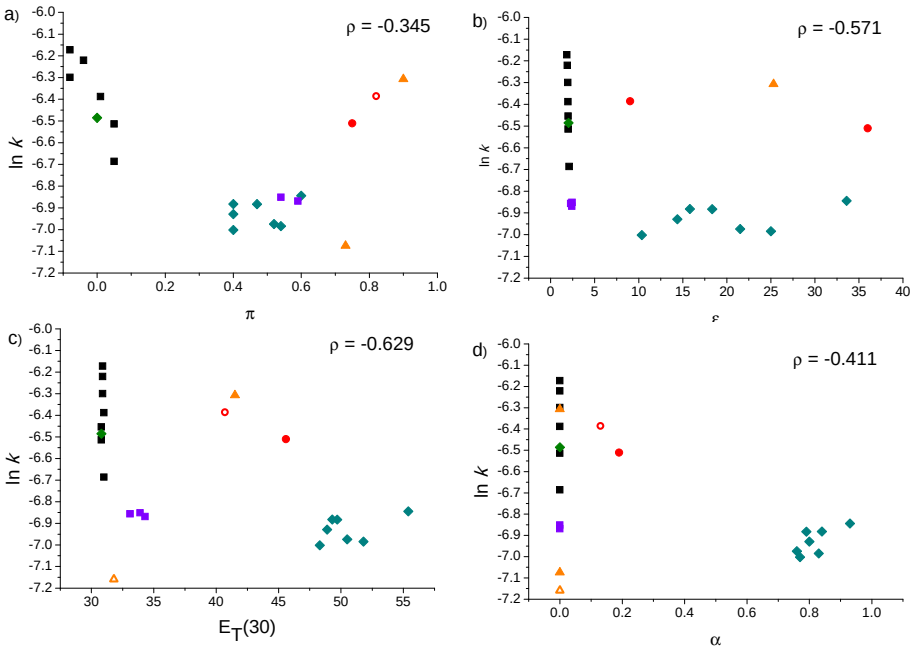

Figure 6.4: Thermal helix inversion of **6.1**; ln *k* plotted against 8 different solvent parameters. (a) The π* polarity scale, (b) dielectric constant, (c) the $E_T(30)$ polarity scale, (d) the Kamlet-Taft parameter for hydrogen bond donating ability α. Spearman's rank correlation coefficient (ρ) indicated on each plot.

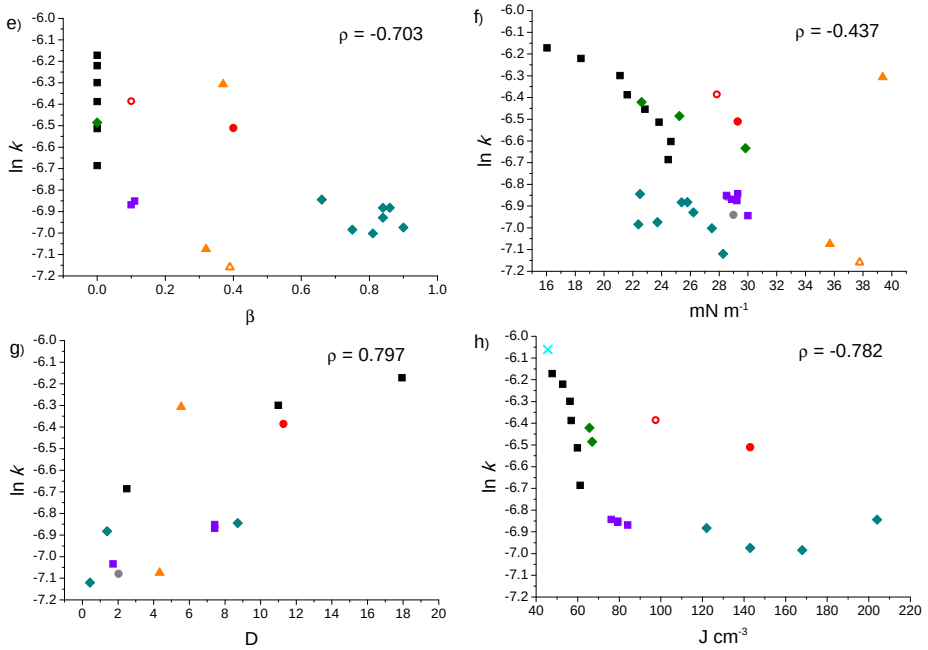

Figure 6.4 (continued): Thermal helix inversion of **6.1**; ln *k* plotted against 8 different solvent parameters. (e) The Kamlet-Taft parameter for hydrogen bond accepting ability β, (f) surface tension, (g) diffusion coefficient, (h) cohesive energy density Spearman's rank correlation coefficient (ρ) indicated on each plot.

In Figure 6.4d and e the parameters plotted are the Kamlet-Taft parameters for hydrogen-bond donating ability and hydrogen bond receiving ability, α and β, respectively, with scales ranging from 0 to 1.[51,52] For example, the aromatic solvents all have β values of up to 0.4 but α values of 0, ruling out any solvent-solvent hydrogen bonding interaction in aromatic solvents. These parameters are 0 for all aliphatic solvents, but approach 1 for the alcohols. For α it is clear that a correlation is absent (ρ = -0.411), however, a noteworthy moderate correlation is observed for β (ρ = -0.703). This relatively high value may be attributed to weak hydrogen bonding of the solvent to the aromatic molecular motor. It has to be noted that this correlation is strongly influenced by the lack of distinction between the aliphatic solvents, which all possess an identical α and β value. Interestingly though, the Kamlet-Taft parameters of the alcohols decrease with an increasing alkyl length, mirroring the convergence of the alcohol trend line with the alkyl trend line (see Figure 6.3). The polar solvents can be found about halfway between the alcohols and most other solvents on the Kamlet-Taft scales.

A reasonable correlation for surface tension was expected, it being strongly related to viscosity (Figure 6.4f).[47] Surprisingly it provided a very weak and insignificant correlation (ρ = -0.437) with most data points spread around the mean. The most notable

feature for this solvent property is the single significant outlier, benzonitrile. This solvent displayed a significant deviation in rate when compared to viscosity. Likewise, benzonitrile deviates when the natural logarithm of the rate is plotted against surface tension. However, in Figure 6.3 this solvent deviates mainly from the aromatics while in Figure 6.4f benzonitrile is an outlier from all other solvents, making the solvent an interesting subject for further studies.

Another property strongly related to viscosity is the diffusion coefficient (D).[53] Furthermore, this property is more attuned to the specific solvent-solute interaction since it is measured specifically for motor **6.1** by DOSY-NMR in several selected solvents (Figure 6.4g).[54] Contrary to surface tension, the diffusion coefficient does exhibit a strong correlation with ln k (ρ = -0.797). This correlation is even stronger than that of viscosity with the rate, also when the viscosity dataset is reduced to the same size as that of the diffusivity. In addition, the Pearson correlation is high, which implies that the rate experiences a stronger linear relationship with the diffusion coefficient than with the viscosity. The high Pearson's r highlights the sensitivity of the diffusion coefficient with respect to solute-solvent interactions, which is to be expected from Kramer's theorem. Consequently, the diffusion coefficient is of the highest interest for future studies. It should be noted that also in this case the incongruity between benzonitrile and anisole persists with both solvents exhibiting similar diffusivities for **6.1**.

Finally, in Figure 6.4h, ln k for selected solvents is plotted against the solvent cohesive energy density.[43,48] This parameter indicates the energy of vaporization, and is a direct reflection of the degree of Van der Waals forces holding the molecules of the liquid together. Since rotation of the motor needs the solvent matrix to rearrange, which requires the Van der Waals interactions between individual solvent molecules to be broken and reformed, this parameter could be very informative. This solvent parameters exhibits a significant and strong correlation (ρ = -0.782), even though it deviates from linearity, as can be seen in Figure 6.4h, with acetonitrile and dichloromethane being the greatest outliers. This parameter does place the aromatic solvents roughly in the right position between the alkanes and alcohols, and due to the curvature it strongly differentiates between the groups. The lack of linearity and the limited amount of liquids for which the cohesive energy density is known makes the interpretation complex and warrants a deeper investigation of the relationship of the reaction rate to this solvent property.

6.5 Statistical analysis

The Pearson's r is appropriate to evaluate the relationship between ln k and ln η since it is expected to be linear. The relationships of other solvent properties with ln k are not required to be linear. The Spearman's ρ is an ideal statistical tool to identify the presence and strength of a monotonic relationship in a dataset (a monotonic function is one that either never increases or never decreases as its independent variable

increases).[55-57] For completeness both statistical parameters were determined with their corresponding probability (Table 6.3). To distinguish significant correlations, the strength of the association ought to be labeled. However, the limits chosen for specific labels are often arbitrary and based on the context of the study.[55] In the current study, association strength is assigned as follows. Any association which explains less than 1/3 of the variance ($\rho < |0.58|$) is labelled as weak, up to 1/2 of the variance ($|0.58| \leq \rho < |0.71|$) as moderate, up to 2/3 of the variance ($|0.71| \leq \rho < |0.82|$) as strong and more than 2/3 ($\rho \geq |0.82|$) as very strong.

Property	Pearson's r	p-value	Spearman's ρ	p-value
ln η	-0.689	**0.000**	**-0.728**	**0.000**
π^*	-0.445	0.043	-0.345	0.126
ε	-0.322	0.155	-0.571	**0.007**
$E_T(30)$	-0.585	**0.004**	-0.629	**0.002**
α	-0.509	0.016	-0.411	0.057
β	-0.640	**0.001**	-0.703	**0.000**
ST	-0.460	**0.009**	-0.437	0.014
D	**0.774**	**0.002**	**0.797**	**0.001**
c.e.d.	-0.632	**0.004**	**-0.782**	**0.000**

Table 6.3: Statistical results of various solvent properties vs ln *k*. Strong correlations as well as significant relationships are bold.

As discussed in the in the previous paragraph, three solvent properties display a significant strong correlation (ln η, c.e.d. and D). It is interesting to note that only the diffusion constant exhibits a strong correlation. It is, however, unreasonable to compare these results directly to oneanother, since the datasets differ in size (Table 6.2). To allow for a fair comparison of the correlation of a solvent property (x) with the natural log of the rate (ln *k*) and the correlation of the natural log of viscosity (ln η) with the natural log of the rate (ln *k*), the data missing from solvent property 'x' was also removed from the 'ln η' dataset, after which the correlations coefficients were calculated again (Table 6.4). The correlation coeffecients for the solvent property 'x' naturally remain unchanged with respect to Table 6.3, as well as their respective p-values. For the modified 'ln η' datasets, all p-values for both correlation coefficients are < 0.01 with one exception (p = 0.012 for Pearson's r of ln η vs ln *k* for property 'D'). The comparison shows that for both the linear as well as the monotonic relationships ln η scores higher than the other solvent properties with the notable exception of the diffusion (D). Not only does the monotonic relationship between the diffusion and the natural log of the rate score higher, so does too the linear relationship.

Property (x)	Pearson's r of x vs ln k	Pearson's r of ln η vs ln k	Spearman's ρ of x vs ln k	Spearman's ρ of ln η vs ln k	R^2 improvement ratio
π*	-0.445	-0.655	-0.345	-0.742	1.22
ε	-0.322	-0.683	-0.571	-0.774	1.05
ET(30)	-0.585	-0.686	-0.629	-0.781	1.11
α	-0.509	-0.662	-0.411	-0.748	1.03
β	-0.640	-0.662	-0.703	-0.748	1.08
ST	-0.460	-0.654	-0.437	-0.711	1.13
D	0.774	-0.674	0.797	-0.764	1.37
c.e.d.	-0.632	-0.749	-0.782	-0.809	1.43

Table 6.4: Statistical results of various solvent properties vs ln k with modified datasets for ln η.

One of the goals of this investigation was to explain the differences found between certain solvent groups for the viscosity dependence of the rate for THI. This explanation was sought after in the presented solvent properties. If, for example, in a certain solvent property the alcohol and aromatic values are grouped separately from the aliphatics, this might provide a reason for the observed difference in viscosity dependence. Since such an explanation was not visually apparent, an attempt was made to provide a quantitized comparison.

The desired 'correction' factor sought after in the additional solvent properties should increase the linearity of the ln η vs ln k relationship. This is expressed in the Pearson's r, though with the data randomly distributed over ln η it is equally well expressed in the coefficient of determination, R^2. The same datasets were used as for the correlation coefficients comparison in Table 6.4. Each set of ln η vs ln k was fitted against eq. 6.2. Eq. 6.2 is a rewritten version of the Eyring equation. The complete derivatization can be found in previously published work,[36] and the parameters c_1-c_6 and d_1-d_4 can be obtained from the experimental results.

$$\ln k = \ln \frac{k_B T}{h} + \frac{d_1 T^3 + d_2 T^2 + d_3 T + d_4}{c_4 T^3 + c_5 T^2 + c_6 T} + \frac{c_1 T^2 + c_2 T + c_3}{c_4 T^2 + c_5 T + c_6} \cdot \ln \eta. \qquad (6.2)$$

Fitting was performed by least squares which provided the R^2's of each dataset. Subsequently the solvent property data was added to each corresponding dataset and using least squares were fitted against eq. 6.3:

$$\ln k = \beta - \alpha \cdot \ln \eta + \gamma \cdot x. \qquad (6.3)$$

in which γ is a correction factor similar to α and x is the corresponding solvent property. There are nearly infinite other possible functions to which ln η and x vs ln k can be fitted using three variables (α, β and γ). However, with the limited available data this would prove to be a fruitless exercise since any random dataset of comparable size

would be provided with a reasonable fit. Therefore we are only interested in the known linear relationship between ln η and ln k on which we investigate a linear correction for x. The least squares analysis provides improved coefficients of determination for (ln η and x vs ln k), which is appropriately compared as the ratio of $(1-R^2_{\ln \eta})/(1- R^2_{x, \ln \eta})$ (Table 6.4). This improvement is to be expected from the addition of $\gamma \cdot x$ since any dataset which deviates from perfect randomness would positively contribute to such a regression. Therefore it is important to evaluate to which extent the correlation has improved after the addition of $\gamma \cdot x$ and to determine whether it is significant. To determine what constitutes a significant improvement of $(1-R^2_{\ln \eta})/(1- R^2_{x, \ln \eta})$, a Monte Carlo analysis was performed which revealed that for these datasets the improvement has to be ≥1.45 in order to fall outside of 99% random improvement (p-value < 0.01). Solely the cohesive energy density, which exhibits a reasonably strong correlation by itself, improves the R^2 ratio sufficiently. Therefore, from this analysis no additional information could be obtained regarding the differences in the solvent groups with respect to the viscosity dependence of the rates. An explanation might be obtained by the use of computational chemistry. In the previous publication a reasonable estimate for the THI barrier could be obtained from DFT calculations. Such calculations can be corrected using solvent models. However, the very subtle manner in which the solvents influence the rate for THI possibly require the inclusion of significant amounts of solvent molecules. Therefore, simulations using classical molecular dynamics might be the most appropriate tool to investigate the solvent shell surrounding the molecular motor as well as solvent-solute interactions. Such a study was deemed beyond the scope of this investigation.

6.6 Conclusions

In conclusion, the rate of an apolar thermal unimolecular process has been measured in 50 different solvents and solvent mixtures. A large overall dependence of the rate on viscosity is clear, which follows preliminary conclusions described in detail in earlier work.[36] This dependence is especially strong for groups of solvents of which other solvent properties remain consistent upon increasing viscosity. These groups exhibit a linear dependence of ln k on ln η. However, the strength of this dependence differs between the series.

The relatively good fit between the overall data set and viscosity shows that solvent-solute interactions are small compared to those in azobenzenes and bis-oxonols. This effect is presumably due to the apolar nature of motor **6.1** used as the solute. Therefore, the proposed model suggests that intermolecular forces in the solvent are the main reason behind this difference. The solvent shell around the solute needs to rearrange upon isomerization of motor **6.1**. When the Van der Waals interactions between these solvent molecules are strong, due to for example hydrogen bonding or π-π interactions, this requires more energy and therefore the thermal process is decelerated. Such effects have not been described previously for unimolecular thermal isomerizations, as rate

change in polar and/or hydrogen bonding solutes is dominated by solvent-solute interactions, which are of a much larger magnitude. The natural logarithm of the rate of rotation was plotted against eight other solvent parameters. Statistical analysis provided a useful insight into the correlation of these solvent parameters with the rate of the THI. A moderate correlation was found with hydrogen bond donating ability of the solvent. However, the overall retained dependence on viscosity indicates only minor solvent-solute interactions. These results provide a markedly different insight in solvent effects on the isomerization process, since hydrogen bonding interactions are typically much stronger. No parameter scale based on π-π interactions could be found. However, as the rate retardation in aromatic solvents could not be explained by any of the other parameters that were compared, it seems likely that these interactions are a relevant factor in the rate retardation of the THI of motor **6.1**. Furthermore, the best correlation was found with the diffusion coefficient and cohesive energy density. As the diffusion coefficient is strongly related to viscosity, these findings can be rationalized. However, the influence of cohesive energy density on the rate of the THI offers an interesting opportunity for further investigation. Additionally, dispersive interactions might play a significant role. In depth computational studies could shed light on such interactions.

Solvent effects comprise a vast range of different interactions, both among the solvent molecules and between solvent and solute. Hence, it is not surprising that the rate change of a unimolecular process in different solvents cannot be simply explained by one or two solvent parameters. It seems rather logical that such an effect is governed by a complex interplay between several distinct properties. It is tempting to draw conclusions based on trends observed within groups of similar solvents. Indeed, statistical analysis based on one solvent group could easily lead to a much higher correlation than any of the values reported in this work. However, this research aims to give a comprehensive overview. This investigation presents not only the most extensive solvent scope performed so far on a thermal unimolecular reaction, but also the consideration of nine different solvent parameters. Despite the complexity of the many possible combinations of solvent interactions, a few parameters that significantly influence the rate of this apolar unimolecular thermal reaction have been identified. This knowledge will be highly relevant in the future design of molecular switches and motors, and the study of more complex dynamic systems.

6.7 Experimental procedures and acknowledgements

This work was executed in collaboration with Jos Kistemaker, MSc. Statistical analysis was performed by dr. Esther Smits. Mathematical derivations were performed by dr. Erik Bloemsma. For general remarks regarding experimental work, see Chapter 2. For characterization of motor **6.1**, see Supporting Information of reference 36.

6.8 References

1 C. Reichardt, T. Welton, *Solvents and Solvent Effects in Organic Chemistry*, Wiley-VCH Verlag GmbH & Co. KGaA, Weinheim, FRG, 2010.
2 O. Tapia, J. Bertrán, *Solvent Effects and Chemical Reactivity*, Kluwer Academic Publishers, Dordrecht, 2002, vol. 17.
3 N. Menshutkin, *Zeitschrift für Phys. Chemie* **1890**, *5*, 589.
4 E. Grunwald, S. Winstein, *J. Am. Chem. Soc.* **1948**, *70*, 846–854.
5 L. P. Hammett, A. J. Deyrup, *J. Am. Chem. Soc.* **1932**, *54*, 2721–2739.
6 E. D. Hughes, C. K. Ingold, *J. Chem. Soc.* **1935**, 244–255.
7 J. D. Moseley, P. M. Murray, *J. Chem. Technol. Biotechnol.* **2014**, *89*, 623–632.
8 J. Raeburn, C. Mendoza-Cuenca, B. N. Cattoz, M. A. Little, A. E. Terry, A. Zamith Cardoso, P. C. Griffiths, D. J. Adams, *Soft Matter* **2015**, *11*, 927–935.
9 J. L. Farmer, R. D. J. Froese, E. Lee-Ruff, M. G. Organ, *Chem. Eur. J.* **2015**, *21*, 1888–1893.
10 G. Litwinienko, A. L. J. Beckwith, K. U. Ingold, *Chem. Soc. Rev.* **2011**, *40*, 2157–2163.
11 L. Shuai, J. Luterbacher, *ChemSusChem* **2016**, *9*, 133–155.
12 A. Nitzan, *J. Chem. Phys.* **1987**, *86*, 2734–2749.
13 G. N. Eyler, A. I. Cañizo, C. M. Mateo, E. E. Alvarez, L. F. R. Cafferata, *J. Org. Chem.* **1999**, *64*, 8457–8460.
14 D. L. Hasha, T. Eguchi, J. Jonas, *J. Am. Chem. Soc.* **1982**, *104*, 2290–2296.
15 Y. Hirata, Y. Kanemoto, T. Okada, T. Nomoto, *J. Mol. Liq.* **1995**, *65/66*, 421–424.
16 C. J. Tredwell, *J. Chem. Soc. Faraday Trans. II* **1980**, *76*, 1627–1637.
17 W. Adam, M. Grüne, M. Diedering, A. V. Trofimov, *J. Am. Chem. Soc.* **2001**, *123*, 7109–7112.
18 W. Adam, V. Mart, C. Sahin, A. V. Trofimov, *Chem. Phys. Lett.* **2001**, *340*, 26–32.
19 W. Adam, A. V. Trofimov, *Acc. Chem. Res.* **2003**, *36*, 571–579.
20 S. E. Greenough, M. D. Horbury, J. O. F. Thompson, G. M. Roberts, T. N. V Karsili, B. Marchetti, D. Townsend, V. G. Stavros, *Phys. Chem. Chem. Phys.* **2014**, *16*, 16187–16195.
21 J. Schroeder, *J. Phys. Condens. Matter* **1996**, *8*, 9347–9387.
22 J. Schroeder, *Ber. Bunsen-Ges. Phys. Chem.* **1991**, *95*, 233–242.
23 M. Lee, A. J. Bain, P. J. McCarthy, C. H. Han, J. N. Haseltine, A. B. Smith III, R. M. Hochstrasser, *J. Chem. Phys.* **1986**, *85*, 4341–4347.
24 H. A. Kramers, *Physica* **1940**, *7*, 284–304.
25 D. Gegiou, K. A. Muszkat, E. Fischer, *J. Am. Chem. Soc.* **1968**, *90*, 12–18.
26 A. K. Doolittle, *J. Appl. Phys.* **1951**, *22*, 1471–1475.
27 K. M. Keery, G. R. Fleming, *Chem. Phys. Lett.* **1982**, *93*, 322–326.
28 K. Gille, H. Knoll, K. Quitzsch, *Int. J. Chem. Kinet.* **1998**, *31*, 337–350.
29 F. Serra, E. M. Terentjev, *Macromolecules* **2008**, *41*, 981–986.
30 A. C. Benniston, A. Harriman, *J. Chem. Soc. Faraday Trans.* **1994**, *90*, 2627–2634.
31 M. M. Pollard, P. V. Wesenhagen, D. Pijper, B. L. Feringa, *Org. Biomol. Chem.* **2008**, *6*, 1605–1612.
32 R. A. van Delden, N. Koumura, A. Schoevaars, A. Meetsma, B. L. Feringa, *Org. Biomol. Chem.* **2003**, *1*, 33–35.
33 J. Chen, J. C. M. Kistemaker, J. Robertus, B. L. Feringa, *J. Am. Chem. Soc.* **2014**, *136*, 14924–14932.
34 J. Hicks, Z. Babarogic, M. Vandersall, K. B. Eisenthal, *Chem. Phys. Lett.* **1985**, *116*, 19–24.
35 M. Klok, L. P. B. M. Janssen, W. R. Browne, B. L. Feringa, *Faraday Discuss.* **2009**, *143*, 319–334.
36 J. C. M. Kistemaker, A. S. Lubbe, E. A. Bloemsma, B. L. Feringa, *ChemPhysChem* **2016**, *17*, 1819–1822.
37 R. Behrends, K. Fuchs, U. Kaatze, Y. Hayashi, Y. Feldman, *J. Chem. Phys.* **2006**, *124*, 144512.

38 R. Daudel, *Quantum Theory of Chemical Reactivity*, Springer Netherlands, Dordrecht, 1973.
39 M. Levitt, M. F. Perutz, *J. Mol. Biol.* **1988**, *201*, 751–754.
40 S. Scheiner, M. Čuma, *J. Am. Chem. Soc.* **1996**, *118*, 1511–1521.
41 M. Cuma, S. Scheiner, *J. Phys. Org. Chem.* **1997**, *10*, 383–395.
42 C. A. Hunter, J. K. M. Sanders, *J. Am. Chem. Soc.* **1990**, *112*, 5525–5534.
43 D. M. Koenhen, C. A. Smolders, *J. Appl. Polym. Sci.* **1975**, *19*, 1163–1179.
44 M. J. Kamlet, J.-L. M. Abboud, M. H. Abraham, R. W. Taft, *J. Org. Chem.* **1983**, *48*, 2877–2887.
45 Y. Marcus, *Chem. Soc. Rev.* **1993**, *22*, 409–416.
46 J. P. Cerón-Carrasco, D. Jacquemin, C. Laurence, A. Planchat, C. Reichardt, K. Sraïdi, *J. Phys. Org. Chem.* **2014**, *27*, 512–518.
47 J. J. Jasper, *J. Phys. Chem. Ref. Data* **1972**, *1*, 841–1009.
48 J. Burke, *AIC B. Pap. Gr. Annu.* **1984**, *3*, 13–58.
49 M. J. Kamlet, J. L. Abboud, R. W. Taft, *J. Am. Chem. Soc.* **1977**, *99*, 6027–6038.
50 K. Dimroth, C. Reichardt, T. Siepmann, F. Bohlmann, *Ann. der Chemie, Justus Liebigs* **1963**, *661*, 1–37.
51 R. W. Taft, M. J. Kamlet, *J. Am. Chem. Soc.* **1976**, *98*, 2886–2894.
52 M. J. Kamlet, R. W. Taft, *J. Am. Chem. Soc.* **1976**, *98*, 377–383.
53 E. Cussler, *Diffusion Mass Transfer in Fluid Systems*, Cambridge University Press, New York, 3rd ed., 1997.
54 B. Antalek, *Concepts Magn. Reson. Part A Bridg. Educ. Res.* **2002**, *14*, 225–258.
55 M. J. Campbell, T. D. V. Swincow, *Statistics at Square One*, Wiley-Blackwell, 11th ed., 2009.
56 C. Spearman, *J. Am. Psychol.* **1904**, *15*, 72–101.
57 G. W. Corder, D. I. Foreman, *Nonparametric Statistics for Non-Statisticians*, John Wiley and Sons Lt., Hoboken, NJ, 2009.